

Near-Infrared Polarimetry of the GG Tauri A Binary System ^{*}

Yoichi Itoh¹, Yumiko Oasa², Tomoyuki Kudo³, Nobuhiko Kusakabe⁴, Jun Hashimoto⁵, Lyu Abe⁶, Wolfgang Brandner⁷, Timothy D. Brandt⁸, Joseph C. Carson⁹, Sebastian Egner³, Markus Feldt⁹, Carol A. Grady^{10,11,12}, Olivier Guyon³, Yutaka Hayano³, Masahiko Hayashi⁴, Saeko S. Hayashi³, Thomas Henning⁷, Klaus W. Hodapp¹³, Miki Ishii³, Masanori Iye⁴, Markus Janson⁸, Ryo Kandori⁴, Gillian R. Knapp⁸, Masayuki Kuzuhara¹⁴, Jungmi Kwon⁴, Taro Matsuo¹⁵, Michael W. McElwain¹⁰, Shoken Miyama¹⁶, Jun-Ichi Morino⁴, Amaya Moro-Martin^{8,17}, Tetsuo Nishimura³, Tae-Soo Pyo³, Eugene Serabyn¹⁸, Takuya Suenaga^{4,19}, Hiroshi Suto⁴, Ryuji Suzuki⁴, Yasuhiro H. Takahashi^{20,4}, Naruhisa Takato³, Hiroshi Terada³, Christian Thalmann²¹, Daigo Tomono³, Edwin L. Turner^{8,22}, Makoto Watanabe²³, John Wisniewski⁵, Toru Yamada²⁴, Satoshi Mayama²⁵, Thayne Currie²⁶, Hideki Takami⁴, Tomonori Usuda⁴, Motohide Tamura^{20,4}

- ¹ Nishi-Harima Astronomical Observatory, Center for Astronomy, University of Hyogo, 407-2, Nishigaichi, Sayo, Hyogo 679-5313, Japan yitoh@nhao.jp
- ² Faculty of Education, Saitama University, 255 Shimo-Okubo, Sakura, Saitama, Saitama 338-8570, Japan
- ³ Subaru Telescope, National Astronomical Observatory of Japan, 650 North A'ohoku Place, Hilo, HI96720, USA
- ⁴ National Astronomical Observatory of Japan, 2-21-1, Osawa, Mitaka, Tokyo, 181-8588, Japan
- ⁵ H.L. Dodge Department of Physics & Astronomy, University of Oklahoma, 440 W Brooks St. Norman, OK 73019, USA
- ⁶ Laboratoire Lagrange (UMR 7293), Université de Nice-Sophia Antipolis, CNRS, Observatoire de la Côte d'Azur, 28 avenue Valrose, 06108 Nice Cedex 2, France
- ⁷ Max Planck Institute for Astronomy, Königstuhl 17, 69117 Heidelberg, Germany
- ⁸ Department of Astrophysical Science, Princeton University, Peyton Hall, Ivy Lane, Princeton, NJ08544, USA
- ⁹ Department of Physics and Astronomy, College of Charleston, 58 Coming St., Charleston, SC 29424, USA
- ¹⁰ Exoplanets and Stellar Astrophysics Laboratory, Code 667, Goddard Space Flight Center, Greenbelt, MD 20771, USA
- ¹¹ Eureka Scientific, 2452 Delmer, Suite 100, Oakland CA96002, USA
- ¹² Goddard Center for Astrobiology
- ¹³ Institute for Astronomy, University of Hawaii, 640 N. Aohoku Place, Hilo, HI 96720, USA
- ¹⁴ Department of Earth and Planetary Sciences, Tokyo Institute of Technology, Ookayama, Meguro-ku, Tokyo 152-8551, Japan
- ¹⁵ Department of Astronomy, Kyoto University, Kitashirakawa-Oiwake-cho, Sakyo-ku, Kyoto, Kyoto 606-8502, Japan
- ¹⁶ Hiroshima University, 1-3-2, Kagamiyama, Higashihiroshima, Hiroshima 739-8511, Japan
- ¹⁷ Department of Astrophysics, CAB-CSIC/INTA, 28850 Torrejón de Ardoz, Madrid, Spain
- ¹⁸ Jet Propulsion Laboratory, California Institute of Technology, Pasadena, CA, 171-113, USA
- ¹⁹ Department of Astronomical Science, The Graduate University for Advanced Studies, 2-21-1, Osawa, Mitaka, Tokyo, 181-8588, Japan

^{*} Based on data collected at Subaru Telescope, which is operated by the National Astronomical Observatory of Japan.

²⁰ Department of Astronomy, The University of Tokyo, 7-3-1, Hongo, Bunkyo-ku, Tokyo, 113-0033, Japan

²¹ Astronomical Institute "Anton Pannekoek", University of Amsterdam, Postbus 94249, 1090 GE, Amsterdam, The Netherlands

²² Kavli Institute for Physics and Mathematics of the Universe, The University of Tokyo, 5-1-5, Kashiwanoha, Kashiwa, Chiba 277-8568, Japan

²³ Department of CosmoSciences, Hokkaido University, Kita-ku, Sapporo, Hokkaido 060-0810, Japan

²⁴ Astronomical Institute, Tohoku University, Aoba-ku, Sendai, Miyagi 980-8578, Japan

²⁵ The Center for the Promotion of Integrated Sciences, The Graduate University for Advanced Studies (SOKENDAI), Shonan International Village, Hayama-cho, Miura-gun, Kanagawa 240-0193, Japan

²⁶ Department of Astronomy & Astrophysics, University of Toronto, 50 George St., Toronto, Ontario, M5S 3H4, Canada

Received 2013 November 29; accepted 2014 May 5

Abstract A high angular resolution near-infrared polarized-intensity image of the GG Tau A binary system was obtained with the Subaru Telescope. The image shows the circumbinary disk scattering the light from the central binary. The azimuthal profile of the polarized intensity of the circumbinary disk is roughly reproduced by a simple disk model with the Henyey-Greenstein function and the Rayleigh function, indicating small dust grains at the surface of the disk. Combined with a previous observation of the circumbinary disk, our image indicates that the gap structure in the circumbinary disk orbits anti-clockwise, while material in the disk orbit clockwise. We propose a shadow of material located between the central binary and the circumbinary disk. The separations and position angles of the stellar components of the binary in the past 20 years are consistent with the binary orbit with $a = 33.4$ AU and $e = 0.34$.

Key words: stars: individual (GG Tauri) — stars: pre-main sequence – techniques: high angular resolution

1 INTRODUCTION

Proto-planetary disks are common structures around classical T Tauri stars. A number of disks have been investigated at various wavelengths. However, many observations have focused on the disks around single stars, while more than half of T Tauri stars are binaries (Ghez et al. 1993; Leinert et al. 1993). Disks around binaries are expected to have forms different from those around single stars. Artymowicz & Lubow (1996) indicated two kinds of disks around a binary system: a circumstellar disk associated with each star and a ring-shaped circumbinary disk around the binary system. A cavity exists between the circumbinary disk and the central binary. Several circumbinary disks have been spatially resolved at the near-infrared wavelengths (e.g. UY Aur; Hioki et al. 2007, FS Tau; Hioki et al. 2011).

GG Tau ($d \sim 140$ pc) is a well-studied young multiple system. The system has two binaries: GG Tau Aa/Ab and GG Tau Ba/Bb. The GG Tau A binary (hereafter GG Tau) is especially interesting, because its circumbinary disk has been spatially resolved at the millimeter wavelengths (Guilloteau et al. 1999), at the near-infrared (Roddier et al. 1996; Itoh et al. 2002), and at the optical (Krist et al. 2002). The large-scale structure of the circumbinary disk is well characterized by an annulus with an inner radius of 190 AU. The disk is inclined by $\sim 37^\circ$ with the northern edge nearest to us. The kinematics of the disk are consistent with clockwise Keplerian rotation (Guilloteau et al. 1999). Duchêne et al. (2004) observed GG Tau at the L' -band ($\lambda = 3.8\mu\text{m}$). Comparing this with shorter wavelength images, they proposed a stratified structure for the circumbinary disk, in which large dust grains are present near the disk midplane. They suggested vertical dust settling and grain growth in the dense part of the disk.

Polarimetric observations also yield insight into dust properties and disk structures. [Tanii et al. \(2012\)](#) carried out near-infrared polarimetry for UX Tau. The circumstellar disk of UX Tau shows large variety in the polarization degree, from 1.6 % up to 66 %. They attributed this large variation to non-spherical large dust grains in the circumstellar disk. This observation confirmed dust growth in a circumstellar disk. On the other hand, several observations suggest small dust grains in proto-planetary disks. [Silber et al. \(2000\)](#) carried out polarimetric observations of GG Tau at 1 μm . They found that the circumbinary disk is strongly polarized, up to ~ 50 %, which is indicative of Rayleigh-like scattering from sub-micron dust grains.

We present the results of near-infrared polarimetry of GG Tau. Combining a coronagraph with an adaptive optics system, we obtained a high spatial resolution polarized-intensity image of GG Tau. The observations and the data-reduction procedure are described in section 2. In section 3, we discuss the circumbinary structures around GG Tau and the orbital motion of the GG Tau binary.

2 OBSERVATIONS AND DATA REDUCTION

Near-infrared H -band (1.6 μm) polarimetric imaging observations of GG Tau A were carried out on September 4, 2011 with the High Contrast Instrument for the Subaru next-generation Adaptive Optics (HiCIAO) and the adaptive optics system, AO188, mounted on the Nasmyth platform of the Subaru Telescope. The observations were conducted as part of the SEEDS survey. We employed the Polarization Differential Imaging (PDI) mode. In this mode, the Wollaston prism installed in HiCIAO divides the incident light into two linearly polarized components, which are perpendicular to each other and imaged simultaneously on the detector. Each image has 1024×2048 pixels with a field of view of $9''.75 \times 20''.09$ and a pixel scale of $9.521 \text{ mas pixel}^{-1}$ in the east-west direction and $9.811 \text{ mas pixel}^{-1}$ in the north-south direction. In the PDI mode, when the half-wave plate is set at an offset angle of 0° , 45° , 22.5° , and 67.5° , we obtained polarimetric images with the polarization direction at 0° and 90° , 90° and 0° , 45° and 135° , and 135° and 45° components, respectively. The full width at half maximum of the point spread function (PSF) was $0''.11$. We used a coronagraphic mask with $0''.6$ diameter to suppress the brightness of GG Tau Aa/Ab. We obtained 64 frames with an exposure time of 30 s for each. We also took short exposure frames without the coronagraphic mask. For a PSF reference star, we took SAO 76661 after the GG Tau observations with the same instrumental configuration except for use of the $0''.3$ diameter coronagraphic mask. We used an ND filter in the AO system to match the R -band magnitudes between GG Tau and SAO 76661 where wavefronts were sensed. Twelve frames were taken with an exposure time of 30 s.

The Image Reduction and Analysis Facility (IRAF¹) software was used for data reduction. We followed reduction procedures given by [Tanii et al. \(2012\)](#). All HiCIAO frames have artifacts of horizontal stripes and vertical bandings. These patterns were removed with a dedicated program. Next, we removed hot and bad pixels and divided the object frames by the flat frame. After these processes, we obtained flux images of the polarimetric components, F_{0° and F_{90° , F_{90° and F_{0° , F_{45° and F_{135° , and F_{135° and F_{45° , separated to the left and right of the image. The Stokes parameters, Q and U , are derived as

$$Q = F_{0^\circ} - F_{90^\circ}, \quad (1)$$

$$U = F_{45^\circ} - F_{135^\circ}. \quad (2)$$

By subtracting the right images from the left images, we obtained 16 images of Q and $-Q$, and 16 images of U and $-U$. We constructed polarized intensity (PI) images by

$$PI = \sqrt{Q^2 + U^2}. \quad (3)$$

Assuming that polarization due to interstellar material in front of GG Tau is negligible, the polarized intensity image represents the polarized components of circumbinary structures.

¹ IRAF is distributed by National Optical Astronomy Observatory, which is operated by the Association of Universities for Research in Astronomy, Inc., under cooperative agreement with the National Science Foundation.

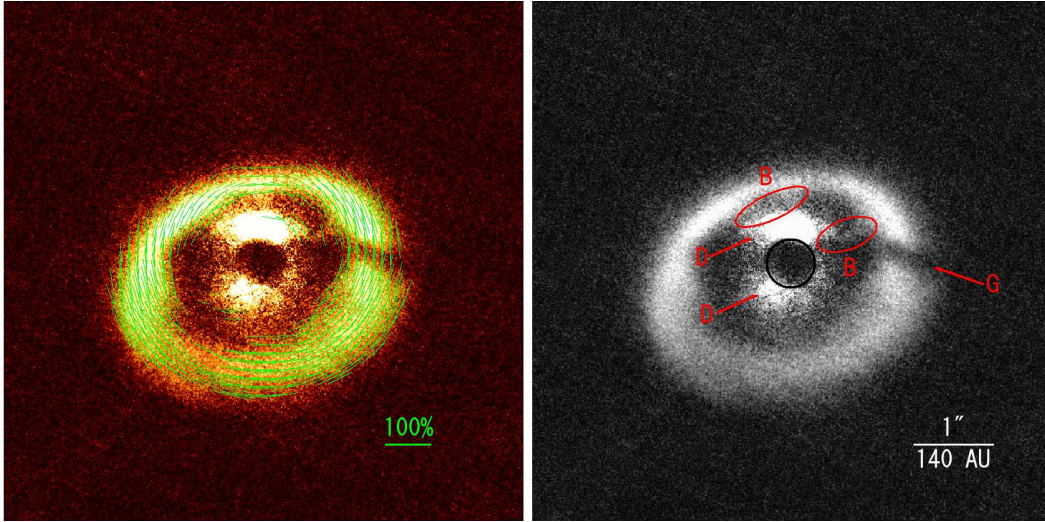


Fig. 1 (left) An H -band polarized intensity image of the GG Tau Aa/Ab binary system. Polarization vectors are overplotted. Degrees and angles of the polarization in an 11×11 pixel box are averaged, if the polarized intensity is detected to more than six σ of the sky and if the degree of each pixel is less than 100%. The field of view is $6''.5 \times 6''.5$. North is up and east toward left. (right) Structures discussed below are indicated on the polarized intensity. G: the gap structure, D: the circumstellar disks, and B: the bridges. The black circle indicates the position of the coronagraphic mask.

To derive the polarization degree, P , of the circumbinary structures, the polarized-intensity image needs to be divided by the intensity image, which contains only the components of the circumbinary structures. The intensity image of GG Tau (hereafter I_{tot}) consists of the intensity of circumbinary structures as well as that of the central binary. By subtracting the intensity image of the central binary (I_*) from I_{tot} , we obtained an intensity image of the circumbinary structure (I_{disk}), i.e., $I_{\text{disk}} = I_{\text{tot}} - I_*$. For I_* , we created a pseudo-binary image by duplicating the images of the PSF reference star. Detailed description of the PSF subtraction is presented in Itoh et al. (2002). Even with the procedure above, we did not subtract PSF of the GG Tau binary perfectly. We attribute this imperfection to a mismatch between the AO corrections of GG Tau and the PSF reference star. As a result, the degrees of polarization have uncertainties as large as 20%. On the other hand, the angle of polarization and polarized intensity are trustworthy, because these two values were obtained before the PSF subtraction.

3 RESULTS AND DISCUSSION

The polarized intensity image of the GG Tau A binary is shown in Figure 1 with the polarization vectors overlaid. The central binary was imaged within the coronagraphic mask with a significant suppression of its light. The ring-shaped circumbinary disk is clearly seen. The polarization degrees of the circumbinary disk are between 30% and 100%.

The gap structure in the circumbinary disk is evident as a sudden dip to the west. We propose three hypotheses for this structure: a less dense region around a planet, a shade made by the circumbinary structure, and a shadow cast by inner material. Numerical simulations indicate that at an early phase of a planetary formation, a less dense region appears around a planet (e.g., Mayer et al. 2004). If the region is optically thin, a gap structure appears in the polarized intensity image of the disk. The less dense region around a planet would orbit the binary with the Keplerian velocity.

We detected the orbital motion of the gap structure, by comparing the image taken in 2001 (Itoh et al. 2002) with that taken in 2011. Because the inclination of the disk is 37° , the positions of the gap structure were measured in the deprojected disk. We defined a box as the gap region, of which two short sides are interpolations of the inner and outer edges of the circumbinary disk. Points at the intersections of these two sides with the middle of the long sides are defined as the reference points of the gap structure. The positions of the reference points are measured from the centroid of the binary. The mass of each component of the binary is $0.78 M_\odot$ and $0.68 M_\odot$, respectively (White et al. 1999). The positions of the binary components were accurately measured in the 2001 image, because the coronagraphic mask has a transmittance of a few tenths of a percent. For the 2011 image, the positions of the binary are measured in the short exposure frames. The separations between the centroid of the binary and the inner reference point of the gap structure were 150 AU at 2001 and 160 AU at 2011. Those of the outer reference point were 240 AU at 2001 and 260 AU at 2011. We consider these discrepancies are due to ambiguous boundaries of the gap region. The position angle (PA) of the inner reference point was $-91^\circ.5$ at 2001 and $-85^\circ.6$ at 2011. That of the outer reference point was $-101^\circ.4$ at 2001 and $-96^\circ.5$ at 2011. Changes in the PAs are $+5^\circ.9$ for the inner reference point and $+4^\circ.9$ for the outer reference point. This change corresponds to the orbital periods of 650 yr and 780 yr, respectively, assuming constant angular velocity. However, the expected orbital periods are 1700 yr for a point at 160 AU from the centroid and 3500 yr for a point at 260 AU. The change in the PA during two observational epochs should be $2^\circ.2$ and $1^\circ.1$ for the inner and outer reference points, respectively. Thus, the change of the position angles of the gap is not consistent with the angular velocity predicted from the Kepler motion of the circumbinary disk.

Moreover, the motion of the gap structure is in a direction opposite that of the disk material. Kawabe et al. (1993) Kawabe (Ishiguro) resolved the circumbinary disk in the millimeter wavelengths. The redshifted component of the ^{12}CO emission is located at west of the dust continuum and the blueshifted component at east. Roddier et al. (1996) observed the GG Tau binary in the near-infrared wavelengths with the adaptive optics system. They revealed the orbital motions of the binary components in the clockwise sense. Assuming that the orbital angular momenta of the stars and the circumbinary disk are roughly in the same direction, Guilloteau et al. (1999) indicated that the material in the circumbinary disk orbit clockwise and the disk is inclined such that its northern edge is nearest to us. On the other hand, comparison of the optical and near-infrared images of GG Tau reveals that the gap structure moves in the opposite direction. In the *HST* optical image taken at 1997, the PA of the gap is -92° (Krist et al. 2002). In the near-infrared image taken at 1998 with *HST* (Silber et al. 2000) and in that taken at 2001 with the Gemini telescope (Potter et al. 2001) the PAs of the gap structure seem around -90° . In the near-infrared image taken at 2001, the PA of the gap structure is $-91^\circ.5$ at the inner reference point and $-101^\circ.4$ at the outer reference point (Itoh et al. 2002). The PAs of the gap structure is $-85^\circ.6$ at the inner reference point and $-96^\circ.5$ at the outer reference point at 2011. These measurements indicate that the motion of the gap structure is anti-clockwise and in a direction opposite that of the disk material. We conclude that the gap structure is not a less dense region around a planet in the circumbinary disk.

Next, we consider a shade made by the circumbinary structure. It is expected that the shade appears as a dark region in the polarized intensity image of the disk, if the disk has a local concave structure. If the circumbinary disk is a rigid body, a local concave, thus a shade, would orbit the binary in a prograde direction. Otherwise, if a retrograde density wave propagates through the circumbinary disk, a shade moves independently of the disk matter. However, spiral density waves in a circumstellar disk can be amplified only if the wave rotates in a prograde sense (e.g. Shu et al. 2000). We claim that the gap structure is not a shade made by a local concave of the circumbinary disk.

Itoh et al. (2002) proposed that the gap structure may be a shadow of a material between the central binary and the circumbinary disk. First, we consider a circumstellar disk of the binary component as an obscuring structure. It is known that the circumbinary disk is a thick flared disk. If the circumstellar disk is largely inclined to the plane of the circumbinary disk, illumination of the central star to the circumbinary disk would be suppressed along the midplane of the circumstellar disk. However, Silber et al. (2000) rejected this hypothesis due to lack of a second, diametrically opposed gap on the circumbinary disk. Krist et al. (2002) proposed a circumstellar disk with a large azimuthal density enhancement. Such an enhancement may shadow the circumbinary disk to produce the gap structure. The PA of the gap

axis should equal the PA of the gap structure, if an obscuring structure is spherical or extends only in the radial direction. However, the PA of the gap axis is -111° , which is very different from the PA of the gap structure. If the obscuring structure extends in the azimuthal direction, the structure can create a shadow whose axis PA is different from the PA of the shadow. A circumstellar disk with an azimuthal density enhancement has been reported around several YSOs (e.g. AB Aur, [Fukagawa et al. 2004](#); V718 Per, [Grinin et al. 2008](#)). The gap structure moves in a retrograde direction. Assuming that the orbital angular momenta of the stars, the circumstellar disks, and the circumbinary disk are roughly in the same direction, a precessing circumstellar disk may account for the shadow. Such a disk is proposed for the circumbinary disk around an eclipsing young system, KH 15D ([Kusakabe et al. 2005](#)). As a conclusion, we propose a precessing circumstellar disk with an azimuthal structure, shadowing a part of the circumbinary disk.

As the obscuring structure other than the circumstellar disk, [Krist et al. \(2002\)](#) proposed a dense clump in an accretion stream. We also imagine that the jet emanating from the secondary star tilts to the circumbinary disk. Dust in the jet blocks a part of the light from the primary star, making a shadow on the circumbinary disk. To identify the obscuring structure, high-spatial resolution observations in close vicinity of the binary system are required.

There are emissions between the binary and the circumbinary disk. Two emissions around the binary extend north and south. Bridge structures are seen with the PA between 0° and 40° and with the PA at -60° , respectively. These structures are not ghosts, because these are polarized. If they are not polarized, no structure appears in the polarized intensity image. The polarization vectors depicted at a part of the structures face the binary, indicating scattering. We consider that the former and latter structures correspond to the circumstellar disks and bridges between the circumbinary disk and the circumstellar disks, respectively. A bridge structure between a circumbinary disk and circumstellar disks is suggested in many numerical simulations (e.g. [Bate & Bonnell 1997](#); [Hanawa, Ochi & Ando 2010](#)). Materials in a circumbinary disk are thought to accrete to circumstellar disks through the bridge structure. The northern bridge may correspond to the millimeter dust streamer ([Piétu et al. 2011](#)). However, because of imperfection of the PSF subtraction, detections of these structures are marginal. Further polarimetric observations are required under stable conditions.

Figure 2 shows the azimuthal profile of the H -band polarized intensity of the circumbinary disk. In the figure, the polarized intensities derived with a simple disk model are also shown. The profile of the polarized intensity is a combination of an intensity profile and a profile of the polarization degree. We used the Henyey-Greenstein function and the Rayleigh function ([White 1979](#)). We employed the disk model proposed by [Guilloteau et al. \(1999\)](#), i.e., the inclination of the disk is 37° , the position angle of the semi-minor axis is 7° , and the disk opening angle is 15° . From intensity profiles of the disk in multi-wavelengths, [Duchêne et al. \(2004\)](#) derived the scattering g parameter of the Henyey-Greenstein function as 0.41 for the best fit and 0.34 – 0.55 for the acceptable values. We calculated the polarized intensities with $g = 0.34, 0.41, \text{ and } 0.55$. The polarized intensity will decrease, if the disk surface ripples, for example. We compared the polarized intensity derived from the disk model with the maximum of the observed polarized intensity at each position angle. Among three models, the model with $g = 0.41$ shows the best fit to the observed polarized intensity. Because the disk is optically thick in the H -band, light from the central star is scattered in the surface of the disk. The observed polarized intensity profile is well reproduced with Rayleigh-like scattering, indicating small particles in the surface layer. [Duchêne et al. \(2004\)](#) proposed a stratified structure. It is claimed that large dust grains settled in the midplane of the disk, and the disk surface is dominated by small dust grains. The azimuthal profile of the observed polarized intensity of the disk is consistent with this two-layer structure. Nevertheless, the discrepancies of the polarized intensity between the observation and the model are rather large. We attribute this mismatch to the use of the simple model. Comparison of the polarization degree between observations and the 3-D disk model with light scattering of non-spherical dusts will reveal dust-size distribution in the circumbinary disk.

The orbital motion of the central binary was also examined. The separation and position angle of the binary at 2011 are 256.0 ± 1.6 mas and -30.9 ± 0.3 in the projected plane. The separation has been almost constant for 20 years. Figure 3 shows the position angles of the binary in the last 20 years. [Beust](#)

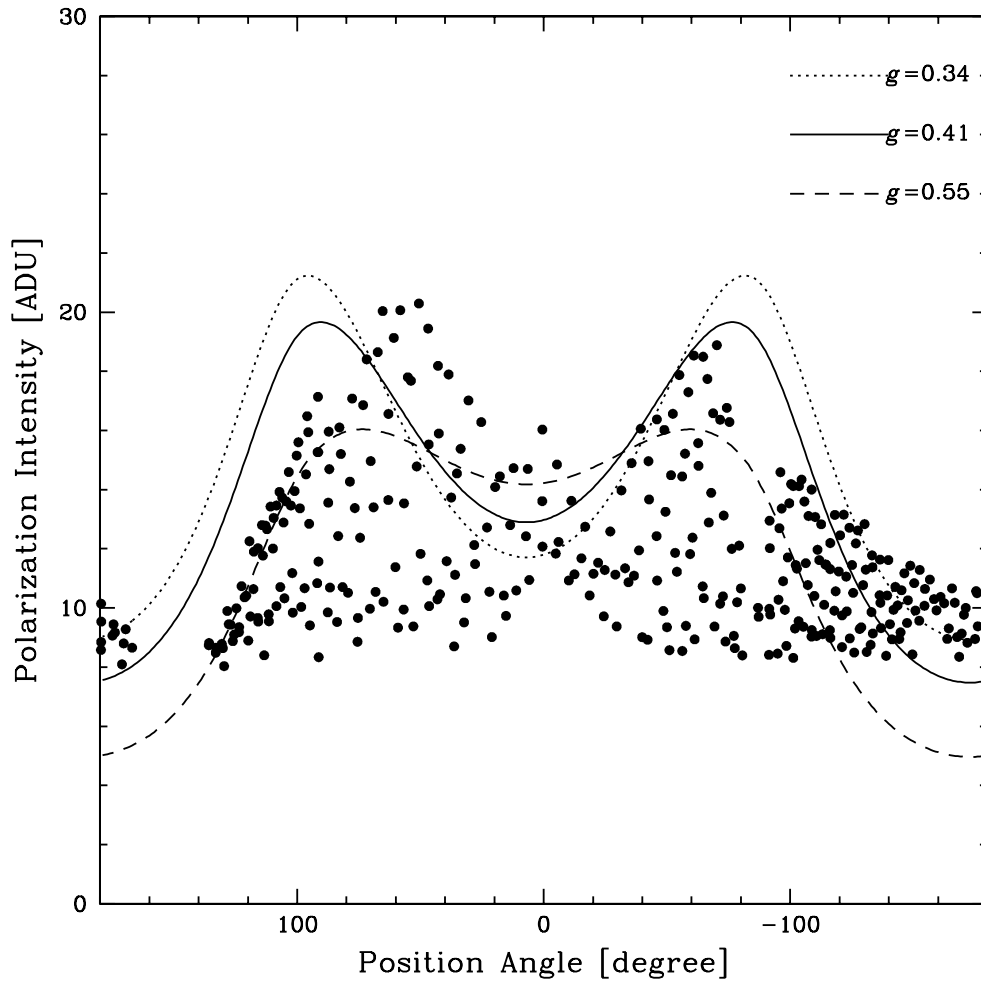


Fig. 2 An azimuthal profile of the polarized intensity of the circumbinary disk of GG Tau. The polarized intensities in an 11×11 pixel box are averaged, if the polarized intensity is detected to more than six σ of the sky and if the degree of each pixel is less than 100%. With this detection threshold, the polarization vectors cover the most region of the circumbinary disk (see Fig. 1). Polarized intensities derived from a simple disk model are shown by lines.

& Dutrey (2005) proposed two orbits for the binary. The small orbit has $a = 33.4$ AU and $e = 0.34$. The large orbit has $a = 62$ AU and $e = 0.35$. The expected position angles for these two orbits are also shown in Figure 3. For the large orbit, the projected separation is as large as 288 mas even at the periastron. For this orbit, we draw the position angles such that the companion passed the periastron at $\text{JD} = 2,450,000$ (circa 1995). The position angle observed in 2011 is consistent with the small orbit, but is not consistent with the large orbit. Beust & Dutrey (2005) and Beust & Dutrey (2006) pointed out that the inner edge of the circumbinary disk is approximately twice as large as should be expected with the small binary orbit. As a cause of this mismatch, they proposed a secular evolution of the GG Tau A orbit and a massive circumbinary planet around ~ 140 AU from the GG Tau A binary.

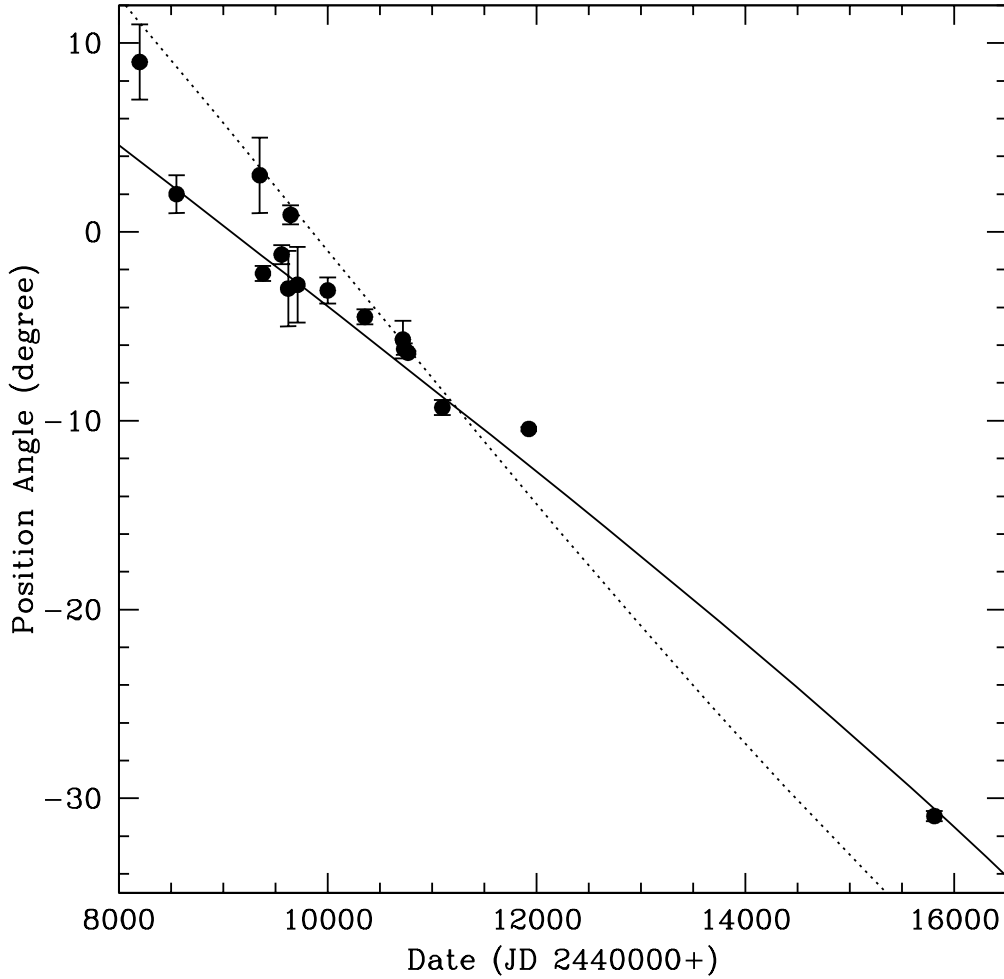


Fig. 3 Position angles of the central binary. The filled circles represent the observed position angles. The solid line indicates the position angles for the orbit with $a = 33.4$ AU and $e = 0.34$. The dotted line indicates the position angles for the orbit with $a = 62$ AU and $e = 0.35$.

4 CONCLUSIONS

A high angular resolution near-infrared polarized-intensity image of the GG Tau A binary system was obtained with the Subaru Telescope.

1. The image shows the circumbinary disk scattering the light from the central binary. Combined with a previous observation of the circumbinary disk, our image indicates that the gap structure in the circumbinary disk orbits anti-clockwise. On the other hand, material in the disk orbit clockwise. We conclude that the gap structure is not a less dense region around a circumbinary planet, nor a shade made by a local concave of the disk, but a shadow of a material located between the binary and the circumbinary disk.

2. The azimuthal profile of the polarized intensity of the circumbinary disk is roughly reproduced by a simple disk model with the Henyey-Greenstein function and the Rayleigh function, indicating small dust grains at the surface of the disk.
3. The separations and the position angles of the stellar components of the binary in the past 20 years are consistent with the binary orbit with $a = 33.4$ AU and $e = 0.34$.

Acknowledgements We thank Dr. Michihiro Takami for useful discussion. Y. I. is supported by a Grant-in-Aid for Scientific Research No. 24540231. J. C. is supported by the U.S. National Science Foundation under Award No. 1009203.

References

- Artymowicz, P., Lubow, S. H. 1996, *ApJ*, 467, L77 2
- Bate, M., Bonnell, I. A. 1997, *MNRAS*, 285, 33 6
- Beust, H., & Dutrey, A. 2005, *A&A*, 439, 585 6, 7
- Beust, H., & Dutrey, A. 2006, *A&A*, 446, 137 7
- Duchêne, G., McCabe, C., Ghez, A. M., Macintosh, B. A. 2004, *ApJ*, 606, 969 2, 6
- Fukagawa, M., Hayashi, M., Tamura, M., et al. 2004, *ApJ*, 605, L53 6
- Ghez, A. M., Neugebauer, G., & Matthews, K. 1993, *AJ*, 106, 2005 2
- Grinin, V., Stempels, H. C., Gahm, G. F., et al. 2008, *A&A*, 489, 1233 6
- Guilloteau, S., Dutrey, A., & Simon, M. 1999, *A&A*, 348, 570 2, 5, 6
- Hanawa, T., Ochi, Y., Ando, K. 2010, *ApJ*, 708, 485 6
- Hioki, T., Itoh, Y., Oasa, Y., et al. 2007, *AJ*, 134, 880 2
- Hioki, T., Itoh, Y., Oasa, Y., et al. 2011, *PASJ*, 63, 543 2
- Itoh, Y., Tamura, M., Hayashi, S. S., et al. 2002, *PASJ*, 54, 963 2, 4, 5
- Kawabe, R., Ishiguro, M., Omodaka, T., et al. 1993, *ApJ*, 404, L63 5
- Krist, J. E., Stapelfeldt, K. R., Watson, A. M. 2002, *ApJ*, 570, 785 2, 5, 6
- Kusakabe, N., Tamura, M., Nakajima, Y., et al. 2005, *ApJ*, 632, L139 6
- Leinert, C., Zinnecker, H., Weitzel, N., et al. 1993, *A&A*, 278, 129 2
- Mayer, L., Quinn, Th., Wadsley, J., Stadel, J. 2004, *ApJ*, 609, 1045 4
- Piétu, V., Gueth, F., Hily-Blant, P., et al. 2011, *A&A*, 528, 81 6
- Potter, D., Baudoz, P., Guyon, O., et al. 2001 *BAAS*, 198, 18.02 5
- Roddier, C., Roddier, F., Northcott, M. J., et al. 1996, *ApJ*, 463, 326 2, 5
- Shu, F. H., Laughlin, G., Lizano, S., Galli, D. 2000, *ApJ*, 535, 190 5
- Silber, J., Gledhill, T., Duchêne, G., Ménard, F. 2000, *ApJ*, 536, L89 3, 5
- Tanii, R., Itoh, Y., Kudo, T., et al. 2012, *PASJ*, 64, 124 3
- White, R. J., Ghez, A. M., Reid, I. M., Schultz, G. 1999, *ApJ*, 520, 811 5
- White, R. L. 1979, *ApJ*, 229, 954 6